Hindawi Publishing Corporation
Mathematical Problems in Engineering
Volume 2014, Article ID 649608, 11 pages
http://dx.doi.org/10.1155/2014/649608

Research Article

Eddy Current Inversion Models for Estimating Dimensions of Defects in Multilayered Structures

Bo Ye,[1] Jun Dong,[1] Gefei Qiu,[1] Siqi Li,[1] Fang Zeng,[1] Tanghua Yang,[2] Biao Bai,[2] and Zhangzhou He[1]

[1] *Faculty of Electric Power Engineering, Kunming University of Science and Technology, Kunming 650500, China*
[2] *Puer Power Supply Bureau, Yunnan Power Grid Corporation, Pu'er 665000, China*

Correspondence should be addressed to Bo Ye; yeripple@hotmail.com

Received 11 December 2013; Accepted 5 February 2014; Published 17 March 2014

Academic Editor: Huaicheng Yan

In eddy current nondestructive evaluation, one of the principal challenges is to determine the dimensions of defects in multilayered structures from the measured signals. It is a typical inverse problem which is generally considered to be nonlinear and ill-posed. In the paper, two effective approaches have been proposed to estimate the defect dimensions. The first one is a partial least squares (PLS) regression method. The second one is a kernel partial least squares (KPLS) regression method. The experimental research is carried out. In experiments, the eddy current signals responding to magnetic field changes are detected by a giant magnetoresistive (GMR) sensor and preprocessed for noise elimination using a wavelet packet analysis (WPA) method. Then, the proposed two approaches are used to construct the inversion models of defect dimension estimation. Finally, the estimation results are analyzed. The performance comparison between the proposed two approaches and the artificial neural network (ANN) method is presented. The comparison results demonstrate the feasibility and validity of the proposed two methods. Between them, the KPLS regression method gives a better prediction performance than the PLS regression method at present.

1. Introduction

Estimating dimensions of defects occurring in multilayered structures is important not only for ensuring the safety of the structural system (e.g., aging nuclear structures, composite aircraft structures, and other civil engineering structures), but also for getting a huge economic benefit from the view of the possible extension of in-service inspection of period [1–3]. To ensure the highest possible operational safety along with economic efficiency, it is necessary to carry out experimental inspections with high sensitivity and reliability. One of the possible solutions of this problem is based on the measurement of magnetic field change generating eddy current (EC) in multilayered structures [4, 5].

Eddy current nondestructive evaluation (ECNDE) is a structure evaluation technique which allows for detecting and characterizing the defects affecting an object without damaging it or altering its functionality [6]. Pioneered by Friedrich Forster in the 1940s, ECNDE as currently practiced is used with electrically conducting materials for various types of measurements. These mainly include measurement of the thickness of metallic plates or nonmetallic coatings on metal substrates, estimation of electrical conductivity or magnetic permeability distributions, and determination of surface and subsurface defect shape and size [7]. However, in point of safety and economic efficiency assessment, there is not too much interest in electrical conductivity and magnetic permeability distributions. The defect dimensions (depth, length, width, and so on) are the main concerns [8]. In ECNDE, the dimensions of defects will be retrieved by inversion of the measured signals [9]. Since the physical model of ECNDE is often complicated and nonlinear, as a result, the inversion model is often ill-posed [10]. In the traditional way, the defect dimensions would be estimated by the analyst visual perception of EC inspection signals [6]. This method usually requires highly trained personnel, and the results are always influenced by the analyst's subjectivity. Then, model-based approaches are used to estimate defect dimensions from EC signals [11]. These methods iteratively solve the forward model to simulate the inspection process and predict the

probe responses. The problem of defect dimension estimation is formulated as an optimization problem, which seeks a set of defect dimensions by minimizing an objective function, representing the difference between the model predicted signals and the measured signals. Such approaches usually involve significant computational efforts, since the physical model needs to be solved repeatedly. Due to their complexity and low speed, the model-based approaches seem not to be suitable for being used to estimate the defect dimensions directly from EC inspection signals. Some researchers begin to turn to the model-free approaches. Initially, the defect dimension estimation problem is treated as a complex statistical pattern recognition problem [12]. These methods usually extract the special properties of defect signals such as shape, phase, peak value, smoothness, convexity, unimodality, or existence of derivatives as the feature vectors. Corresponding defect dimensions are discretized into a set of class labels. The defect dimensions are obtained from the classification of the currently collected signals based on the extracted features. The classification methods yield discrete values instead of continuous values, which lead to insufficiently accurate results. Then, Popa and Miya [13] and Yusa et al. [14] present an artificial neural network (ANN) method to estimate crack depth and reconstruct crack depth profile from EC signals. Davoust et al. [15] propose to use the bilinear regression and ANN methods to estimate flaw size. Rosa et al. [16, 17] use the probability density function estimation methods for defect dimension estimation. They employed sample techniques such as Markov Chain Monte Carlo (MCMC) and Bootstrap methods for estimation of probability density function of defect dimensions to obtain not only the quantity but also the uncertainly characterization of the measurand. Krzywosz [18] applies a multivariate linear regression algorithm to establish the relationship between the inside diameter pit depth and three features (frequency, amplitude, and phase angle) of EC inspection signals. Bernieri et al. propose a model-free method for the reliable estimation of crack shape and dimensions based on the integration of an EC instrument and a support vector machine (SVM) processing algorithm [19]. Among these methods, ANN is an efficient nonlinear statistical data modeling tool, but it usually requires a number of prior knowledge, space limitations, and database of defect signals for neural network training. The multivariate linear regression method can establish a direct and compact model. However, such method often fails to arrive at a sufficient accurate estimation due to the natural nonlinearity of the magnetic field distribution in complex multilayered structures. The probability density function estimation methods have a great problem that sample techniques require much computational time. Although the results SVM method present are quite impressive, the main drawback of SVM is that solving the problem requires an optimization with a complexity that varies at least quadratically with the number of training examples, which becomes intractable in large scale problems. Therefore, a general framework for defect dimension estimation from EC signals is very desirable, which can not only rapidly but also accurately carry out the dimensions of defects in multilayered structures.

This paper presents a general robust procedure for estimating dimensions of defects in multilayered structures from EC signals. Here, a novel EC testing technique with a giant magnetoresistive (GMR) sensor is used to enhance the sensitivity and spatial resolution of the measurement [20]. Since electromagnetic sensor based on GMR effect is sensitive to the magnitude of the magnetic field, the GMR-based EC probe can perform better than the conventional probe for low-frequency applications, that is, when detecting defects deeply buried in multilayered structures. During scanning inspection, eddy currents are induced in multilayered structures as a result of the application of an alternating magnetic field. In the presence of defects, the output voltage variation of the sensor is usually detected as the magnitude perturbations of the magnetic field. This special property of the GMR sensor will lead to a simplified signal conditioning circuit. Theoretically, there is a relationship between defect dimensions and GMR sensor response. In practice, however, this relationship is influenced by noises and many other factors. Therefore, the original signals are preprocessed by wavelet packet analysis (WPA) for noise elimination [21]. Then, two approaches are proposed to find the relationship between defect dimensions and GMR sensor's output voltage, respectively. The first one is a partial least squares (PLS) regression method [22, 23]. The second approach consists in generalizing the kernel method into PLS (kernel partial least squares KPLS) regression [24, 25]. In the second method, the original inputs are mapped into a high-dimensional space using a kernel method. The PLS regression is calculated in the high-dimensional space. Then, we will obtain a nonlinear regression model in the original input space. Finally, the estimation results are given using two methods and compared with those of the ANN method, in terms of estimation accuracy, generalization capability, and robustness, respectively. The ANN approach is employed in ECNDE in order to perform a nonlinear statistical regression. It is very simple and used as a benchmark for the proposed two quantitative evaluation methods. Experimental results show that the proposed two methods present further advances including good generalization capability, robustness of the results, avoidance of overfitting, and low computational burden.

The remainder of the paper is organized as follows. Section 2 gives the general formulation of the problem of dimension estimation of defects in multilayered structures. Section 3 briefly surveys signal denoising technique using the wavelet packet analysis (WPA) method. Section 4 describes two approaches used to estimate the defect dimensions. Section 5 presents the measurement system configuration and the experimental results. Finally, Section 6 contains conclusions.

2. Problem Description

The EC inverse problem here can be described as the task of quantitative estimating dimensions of defects in multilayered structures, where the measured EC signals are given and the unknown dimensions of defects require estimation [26]. During the probe moving over the defect, the output signal of the GMR sensor is produced, which is proportional to the

magnitude perturbations of the magnetic field. The sensor's output signal is

$$\mathbf{X} = K\dot{B}, \tag{1}$$

where $\mathbf{X} = (x_1, x_2, \ldots, x_N)$ is the sensor's output voltage, N is the number of sample points during the scanning inspection, K is the proportionality coefficient, and $\dot{B}$ is magnetic induction intensity. The unknown defect dimensions $\mathbf{Y} = (y_1, y_2, \ldots, y_M)$ have to be estimated from a set of observed signals $\mathbf{X}$. M is the number of dimension variables. The relationship between GMR sensor's output voltage and defect dimensions can be given by the classical regression model:

$$\mathbf{Y} = f(\mathbf{X}, \boldsymbol{\theta}) + \mathbf{E}, \tag{2}$$

where function $f(\cdot)$ describes the relationship between defect dimensions and GMR sensor's output voltage, $\boldsymbol{\theta}$ is the unknown parameter vector, and $\mathbf{E}$ is an error term. The parameter estimation techniques are needed to learn the unknown parameter vector $\boldsymbol{\theta}$ from the real experimental data which contain observations for the calibrated defects (defects with known dimensions). Then, we can construct the relationship $f(\cdot)$ using these parameters. Thus, a general inversion model is obtained. We can use this model to predict the defect dimensions given the acquired EC inspection signals.

Finally, to compare the accuracy and efficiency of the inversion models, several measures of a model's ability to fit data and predictive power are introduced [27]. All of these measures provide an estimate of the average deviation of the model from the data. The root mean square error (RMSE) of the residuals is defined as

$$\mathrm{RMSE} = \sqrt{\frac{\sum_{i=1}^{n} \left(\mathbf{Y}_i - \widehat{\mathbf{Y}}_i\right)^2}{n}}, \tag{3}$$

where $\mathbf{Y}_i$ is the actual value, $\widehat{\mathbf{Y}}_i$ is the predicted value, and n is the total number of samples. The RMSE is termed the root mean square error in calibration (RMSEC) for the training (calibration) set and the root mean square error in prediction (RMSEP) for the testing set.

Another measure of the model fit to the training data is the coefficient of determination R^2, defined as

$$R^2 = 1 - \frac{\mathrm{RSS}}{\mathrm{SS}}, \tag{4}$$

where RSS is the residual sum of squares and SS is the sum of squares of the response variable $\mathbf{Y}$ corrected for the mean. The R^2 indicates the strength of statistical correlation between actual values and predicted values for the model. A model fits the data perfectly if a value of R^2 is higher than 0.9. R^2 between 0.8 and 0.9 indicates that the model fits the data well. R^2 between 0.6 and 0.8 is considered a useful representation of the data, whereas R^2 between 0.5 and 0.6 indicates a poor representation of the data.

The same test can be used for the values predicted from the testing set, Q^2. Consider

$$Q^2 = 1 - \frac{\mathrm{PRESS}}{\mathrm{SS}}, \tag{5}$$

where PRESS is the prediction error sum of squares and SS is the sum of squares of the response variable $\mathbf{Y}$ corrected for the mean. The Q^2 indicates how well the model predicts new data. Usually, R^2 for a training set is larger than Q^2 for a testing set, since calibration models can easily lead to overfitting of the data. A large Q^2 ($Q^2 > 0.5$) indicates the good predictive ability.

3. Signal Preprocessing

In the process of EC inspection, the GMR sensor's output signals may be corrupted by noises and other artificial signals, arising from lift-off, edge effects, high frequency, probe angle variations, and so forth, resulting in unreliable detection and inaccurate characterization of defect dimensions. In order to remove the influence of noise and extract the amplitude of the main components from the measurements, a number of preprocessing steps are required before the defect dimension estimation is possible [21].

WPA [28, 29] has proved its great capabilities in decomposing, denoising, and signal analysis, which makes the analysis of nonstationary signals achievable as well as detecting transient feature components, since wavelet can concurrently impart time and frequency structures. In wavelet packet framework, wavelet packets offer a more complex and flexible analysis, because, in WPA, the details as well as the approximations are split. Before denoising, the GMR sensor's output signals are processed by normalizing so that they have means of zero and standard deviations of 1. Then, the WPA denoising procedure is implemented as in the following four steps.

(1) Decomposition: for a given wavelet, compute the wavelet packet decomposition of signal $f(t)$ at level m.

(2) Computation of the best tree: for a given entropy, compute the optimal wavelet packet tree. Of course, this step is optional.

(3) Threshold of wavelet packet coefficients: for each packet (except for the approximation), select a threshold and apply it to coefficients. In general, the threshold will be refined by trial and error so as to optimize the results to fit particular analysis and design criteria.

(4) Reconstruction: compute wavelet packet reconstruction based on the original approximation coefficients at level m and the modified coefficients.

In this paper, the mother wavelet chosen for simplifying the implementation is the Daubechies 4 wavelet due to the nonsymmetric shape of its wavelet function, which is the best adjustable to the transient nature of EC inspection signals. Using the signal to noise ratio (SNR) and RMSE as a criterion, the WPA denoising effect comparison using a real signal from the scanning inspection of a subsurface rectangular defect (length 5 mm, width 1 mm, height 1 mm, and depth 4 mm) in an aluminum sample is shown in Table 1. The results show that the WPA method with Shannon entropy threshold is superior for EC signal denoising. Figure 1 shows the performance of the WPA denoising method with Shannon entropy threshold using the same signal and the comparison

Table 1: De-noising effect comparison of different WPA methods.

Threshold rules	Shannon	Norm	Energy	Thre
SNR (db)	52.822	49.211	49.985	47.938
RMSE	0.00203	0.00271	0.00253	0.00323

with that of the mean filtering algorithm. In mean filtering algorithm denoising, the SNR and RMSE of the same signal calculated are 32.676 db and 0.01167, respectively. The signal denoising effect using the WPA method is significantly better than the use of mean filtering algorithm.

4. Defect Dimension Estimation Approaches

4.1. Partial Least Squares Regression. PLS regression [22, 23] is a wide class of methods for modeling relationships between sets of observed variables by means of latent variables (components and score vectors). It was first introduced by the Herman Wold and gained popularity in chemometrics research and later industrial applications [30]. In ECNDE, the samples are often difficult to obtain for constructing the inversion model. PLS regression has the advantage of allowing more variables than samples in the data and dealing in a natural way with collinearity. In this case, the solution of the classical least squares method does not exist or is unstable and unreliable. Furthermore, PLS regression allows graphical display of the latent variable space in terms of plots and also interactive diagnostic exploration of the data. Unlike the principal component regression method, PLS regression chooses the latent variables in such a way as to provide maximum correlation with dependent variables. Thus, PLS model contains the smallest necessary number of latent variables. These special properties make the PLS approach more appropriate for modeling the ECNDE inverse problem [31].

In the estimation of defect dimensions, PLS regression is used to find the fundamental relationship between two matrices, $\mathbf{X}$ and $\mathbf{Y}$. Denote by $\mathbf{X} \subset R^N$ an N-dimensional space of variables representing the GMR sensor's output voltage and similarly by $\mathbf{Y} \subset R^M$ an M-dimensional space representing the defect dimensions. After observing n samples from each block of variables, the PLS decomposes the $(n \times N)$ matrix of variables $\mathbf{X}$ and the $(n \times M)$ matrix of variables $\mathbf{Y}$ into the forms

$$\begin{aligned} \mathbf{X} &= \mathbf{U}\mathbf{P}^T + \mathbf{E}, \\ \mathbf{Y} &= \mathbf{V}\mathbf{Q}^T + \mathbf{F}, \end{aligned} \tag{6}$$

where $\mathbf{U}$ and $\mathbf{V}$ are $(n \times p)$ matrices of the p extracted latent vectors, the $(N \times p)$ matrix $\mathbf{P}$ and the $(M \times p)$ matrix $\mathbf{Q}$ represent matrices of loadings, the $(n \times N)$ matrix $\mathbf{E}$ and the $(n \times M)$ matrix $\mathbf{F}$ are the matrices of residuals, and the superscript T denotes the transpose of matrix. The nonlinear iterative PLS algorithm is implemented as follows [31].

Step 1. Randomly initialize $\mathbf{v}$ as any column of $\mathbf{Y}$.

Step 2. Let $\mathbf{w} = \mathbf{X}^T\mathbf{v}$.

Step 3. Let $\mathbf{u} = \mathbf{X}\mathbf{w}$, $\mathbf{u} \leftarrow \mathbf{u}/\|\mathbf{u}\|$.

Step 4. Let $\mathbf{c} = \mathbf{Y}^T\mathbf{u}$.

Step 5. Let $\mathbf{v} = \mathbf{Y}\mathbf{c}$, $\mathbf{v} \leftarrow \mathbf{v}/\|\mathbf{v}\|$.

Step 6. Iterate Step 2~Step 5 until convergence or the maximum number of iterations is reached.

Step 7. Calculate the deflation of $\mathbf{X}$ and $\mathbf{Y}$matrices: $\mathbf{X} \leftarrow \mathbf{X} - \mathbf{u}\mathbf{u}^T\mathbf{X}$, $\mathbf{Y} \leftarrow \mathbf{Y} - \mathbf{u}\mathbf{u}^T\mathbf{Y}$.

Step 8. Go to Step 1 to calculate the next latent variable.

Note that a minor difference of this algorithm from the classical PLS algorithm is that the modified PLS algorithm normalizes the latent vectors $\mathbf{u}$, $\mathbf{v}$ rather than the weight vectors $\mathbf{w}$ and $\mathbf{c}$. After the extraction of the p latent vectors, we can create the $(n \times p)$ matrices $\mathbf{U}$ and $\mathbf{V}$, the $(N \times p)$ matrix $\mathbf{W}$, and the $(L \times p)$ matrix $\mathbf{C}$ consisting of the columns created by the vectors $\{\mathbf{u}_i\}_{i=1}^p$, $\{\mathbf{v}_i\}_{i=1}^p$, $\{\mathbf{w}_i\}_{i=1}^p$ and $\{\mathbf{c}_i\}_{i=1}^p$, respectively, extracted during the individual iterations. The PLS regression model can be expressed with regression coefficient $\mathbf{B}$ and residual matrix $\mathbf{R}$ as follows:

$$\begin{aligned} \mathbf{Y} &= \mathbf{X}\mathbf{B} + \mathbf{R}, \\ \mathbf{B} &= \mathbf{X}^T\mathbf{V}\left(\mathbf{U}^T\mathbf{X}\mathbf{X}^T\mathbf{V}\right)^{-1}\mathbf{U}^T\mathbf{Y}. \end{aligned} \tag{7}$$

To avoid overfitting the training data and obtain a model with good predictive ability, in practice, the selection of the optimal number of PLS components is needed to be carried out. The optimum number of components is usually determined via cross-validation [32]. The cross-validation is often performed on the calibration samples, which has become the standard in PLS regression analysis. During the cross-validation, the model increases one PLS component until the prediction on the calibration samples shows that further PLS components do not improve predictive ability. In this work, the cross-validation is performed by leaving out one sample at a time. In leave-one-out cross-validation, the prediction error sum of squares (PRESS) and the residual sum of squares (SS) are computed and collected. The ratio $\mathrm{PRESS}_h/\mathrm{SS}_{h-1}$ is calculated after each component, and a component is judged to be significant if this ratio is smaller than around 0.95^2. This is often reexpressed as $Q_h{}^2 = 1 - \mathrm{PRESS}_h/\mathrm{SS}_{h-1} \geq (1 - 0.95^2) = 0.0975$ for all $\mathbf{Y}$-variables. Here h is the number of components used in a PLS model.

4.2. Kernel Partial Least Squares Regression. Recently, Kernel methods have become an increasingly popular tool for machine learning tasks such as classification, regression, and novelty detection. The notion of kernels has drawn much interest as it allows one to obtain nonlinear algorithms from linear ones. The attractiveness of such algorithms stems from their efficiency in high-dimensional nonlinear problems and their easy implementation because there are few free parameters to adjust, and the architecture does not need to be found

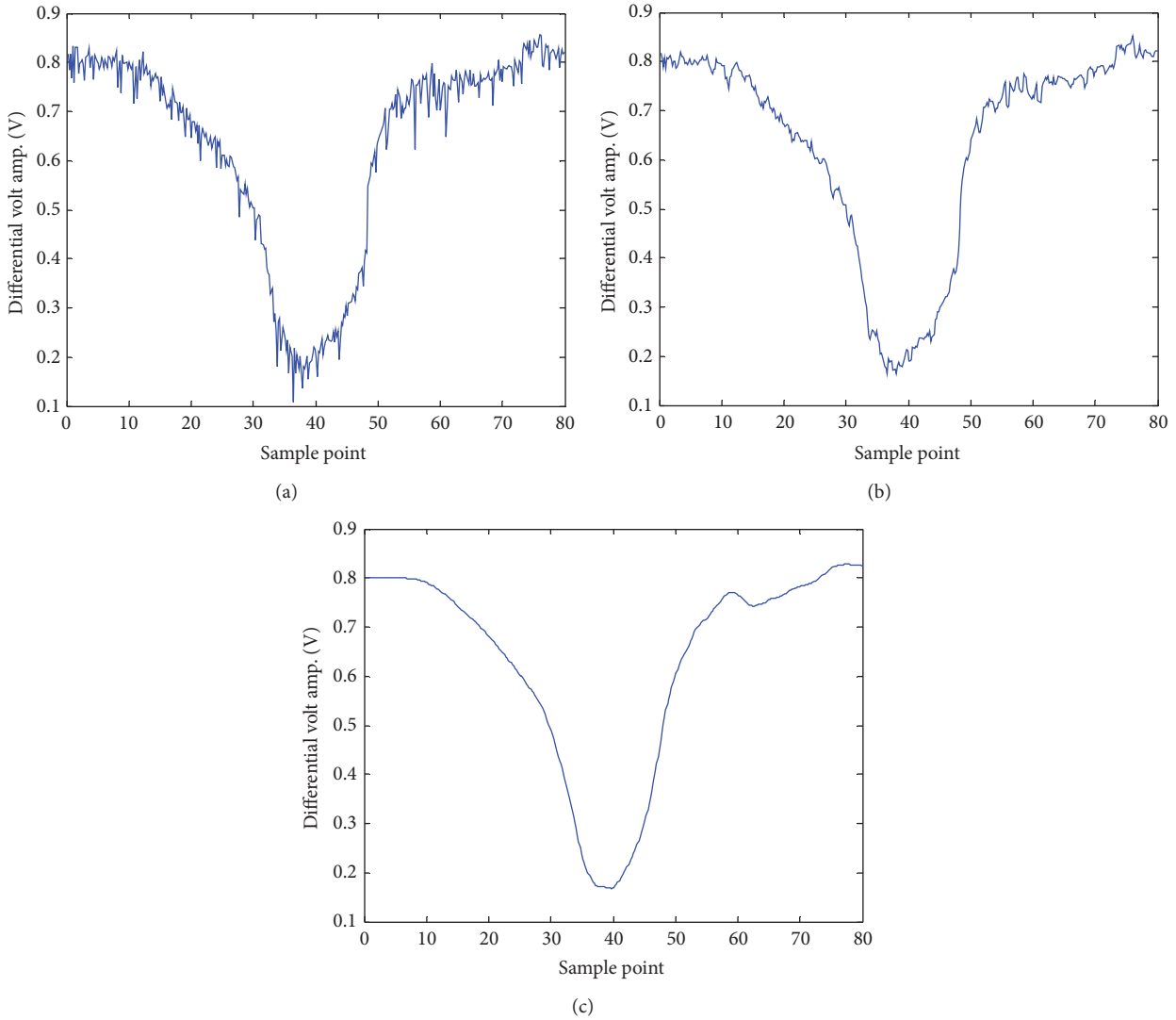

FIGURE 1: The comparison of denoising performance: (a) the original EC signal, (b) the output of denoising using the mean filtering algorithm, and (c) the output of denoising using the WPA method.

by experimentation [33]. It is well known that the estimation of defect dimensions from EC signals is an important aspect of the ECNDE inverse problem which is often nonlinear in realistic inspection. The defect dimension estimation procedures can benefit from a kernel perspective, making them more powerful and applicable to nonlinear processing.

KPLS regression [24, 25] is one type of nonlinear PLS regression developed by generalizing the kernel method into the PLS regression. It can be used to model nonlinear EC data relations. The KPLS regression is presented by Rosipal and Trejo [24]. Specifically, it firstly maps the original inputs into a high-dimensional feature space using the kernel method and then calculates the PLS regression in the high-dimensional feature space to find the fundamental relationships between two matrices ($\mathbf{X}$ and $\mathbf{Y}$). Thus, it means that we can obtain a nonlinear regression model in the space of the original input variables [25].

Now, consider a nonlinear transformation of $\mathbf{X}$ into a feature space F:

$$\mathbf{X} \in R^N \longrightarrow \phi(\mathbf{X}) \in F, \tag{8}$$

where $\phi(\cdot)$ is a nonlinear mapping function that projects the input vectors from the input space to F and $\sum_{i=1}^{N} \phi(x_i) = 0$. Denote by $\boldsymbol{\phi}$ the $(n \times S)$ matrix whose ith row is the vector $\phi(\mathbf{X}_i)$ in an S-dimensional feature space F. The KPLS algorithm directly derived from the PLS algorithm is shown as follows.

Step 1. Randomly initialize $\mathbf{v}$ as any column of $\mathbf{Y}$.

Step 2. Let $\mathbf{u} = \boldsymbol{\phi}\boldsymbol{\phi}^T\mathbf{v} = \mathbf{K}\mathbf{v}$, $\mathbf{u} \leftarrow \mathbf{u}/\|\mathbf{u}\|$.

Step 3. Let $\mathbf{c} = \mathbf{Y}^T\mathbf{u}$.

Step 4. Let $\mathbf{v} = \mathbf{Yc}$, $\mathbf{v} \leftarrow \mathbf{v}/\|\mathbf{v}\|$.

Step 5. Iterate Step 2~Step 4 until convergence or the maximum number of iterations is reached.

Step 6. Calculate the deflation of $\mathbf{K}$ and $\mathbf{Y}$ matrices: $\mathbf{K} \leftarrow (\mathbf{I} - \mathbf{uu}^T)\,\mathbf{K}\,(\mathbf{I} - \mathbf{uu}^T)$, $\mathbf{Y} \leftarrow \mathbf{Y} - \mathbf{uu}^T\mathbf{Y}$.

Step 7. Go to Step 1 to calculate the next latent variable.

Note that $\mathbf{K}$ is the kernel matrix and $\boldsymbol{\phi}\boldsymbol{\phi}^T$ represents the $(n \times n)$ kernel matrix $\mathbf{K}$ of the inner dot products between all mapped input data points $\phi(\mathbf{X}_i)$, $i = 1, \ldots, n$. That is, $\mathbf{K}(\mathbf{X}_i, \mathbf{X}_j) = \phi(\mathbf{X}_i) \cdot \phi(\mathbf{X}_j)$. As the calculations of the dot product $\phi(\mathbf{X}_i) \cdot \phi(\mathbf{X}_j)$ are all replaced with the kernel function $\mathbf{K}(\mathbf{X}_i, \mathbf{X}_j)$, the mapping of $\phi(\mathbf{X}_i)$ from $\mathbf{X}_i$ is implicit. The elegance of using $\mathbf{K}$ is that one can deal with $\phi(\mathbf{X}_i)$ of arbitrary dimensionality without having to compute $\phi(\mathbf{X}_i)$ explicitly. The matrix of regression coefficient $\mathbf{B}$ in the KPLS algorithm will have the form

$$\mathbf{B} = \boldsymbol{\phi}^T\mathbf{V}\left(\mathbf{U}^T\mathbf{KV}\right)^{-1}\mathbf{U}^T\mathbf{Y}. \tag{9}$$

As a result, the predictions on training subset and testing subset can be made as follows, respectively:

$$\begin{aligned} \widehat{\mathbf{Y}} &= \boldsymbol{\phi}\mathbf{B} = \mathbf{KV}\left(\mathbf{U}^T\mathbf{KV}\right)^{-1}\mathbf{U}^T\mathbf{Y}, \\ \widehat{\mathbf{Y}}_t &= \boldsymbol{\phi}_t\mathbf{B} = \mathbf{K}_t\mathbf{V}\left(\mathbf{U}^T\mathbf{KV}\right)^{-1}\mathbf{U}^T\mathbf{Y}, \end{aligned} \tag{10}$$

where $\boldsymbol{\phi}_t$ is the mapped matrix of the testing subset and $\mathbf{K}_t$ is the corresponding kernel matrix. Note that both $\mathbf{K}$ and $\mathbf{K}_t$ should also be mean-centered in feature space before applying (10).

In KPLS, just like other kernel methods, any function satisfying Mercer's condition can be used as the kernel function. Two typical kernel functions are listed below:

$$\begin{aligned} &\text{Polynomial:} \quad \mathbf{K}\left(\mathbf{X}_i, \mathbf{X}_j\right) = \left(\mathbf{X}_i \cdot \mathbf{X}_j + 1\right)^d, \\ &\text{Radial Basis Function:} \quad \mathbf{K}\left(\mathbf{X}_i, \mathbf{X}_j\right) = \exp\left(\frac{-\left\|\mathbf{X}_i - \mathbf{X}_j\right\|^2}{2\sigma^2}\right). \end{aligned} \tag{11}$$

Finally, the cross-validation technique is similarly applied to select the appropriate components which will help avoid overfitting caused by the use of too large dimensional models.

5. Experiments and Results

5.1. Measurement System Configuration. The automatic system based on ECNDE for estimating dimensions of defects in multilayered structures is obtained by integrating the test device with a computer. A block scheme of the system is shown in Figure 2. The system consists of a few main components: an AC excitation generator, two eddy current probes (an inspecting probe and a reference probe), a low pass filter, a data acquisition interface (A/D converter), a coordinate measuring machine (CMM), and a computer. The sinusoidal current source provides current through coils with amplitude 1 A at a frequency 200 Hz. In the system the right-cylindrical air-cored coil probe has been used. The coil parameters are inner radius $r_1 = 3$ mm, outer radius $r_2 = 4.5$ mm, length $l = 20$ mm, and lift-off = 0.5 mm. The probes consist of exciting coils and GMR sensors. The basic AA-Series GMR sensors from Nonvolatile Electronics, Inc. (NVE) are general-purpose magnetometers for use in a wide variety of ECNDE applications. In all subsequent experiments, the AA002-02 GMR sensor is used, due to its' excellent linearity, high sensitivity and resolution, stable and linear temperature characteristics, and a purely ratiometric output. The probes are scanned over the surface of the specimen by using a CMM. A computer program is used to set the scan area and velocity. During measurements, the sensing axis of the GMR sensor is directed orthogonally to the magnetic field generated by the coil. The GMR sensor's output signals are amplified by a low cost, high accuracy instrumentation amplifier AD620. Then, the amplified signals are filtered by a second-order low pass filter with a cutoff frequency of 20 Hz. A data acquisition program written in Labview collects the data from the output of the filter via a National Instrument DAQPad 6016 16 × 6 bit analog-to-digital converter. The computer is controlling the whole system and performing such tasks as automating the process of inspection, data acquisition and displaying, and applying some signal processing techniques to automate the process of defect detection and quantification. The computer-based system can thus increase the reliability of the detection and enhance the performance of EC inspection of complex engineering structures by avoiding errors related to human factors such as inexperience and inconsistency. It also offers fast and robust database methods for retrieving old inspection data, which is important in monitoring defect initiation and growth. In the system, reference structures and a reference probe have been used. By comparing the signals from the reference structures with those from the monitored special

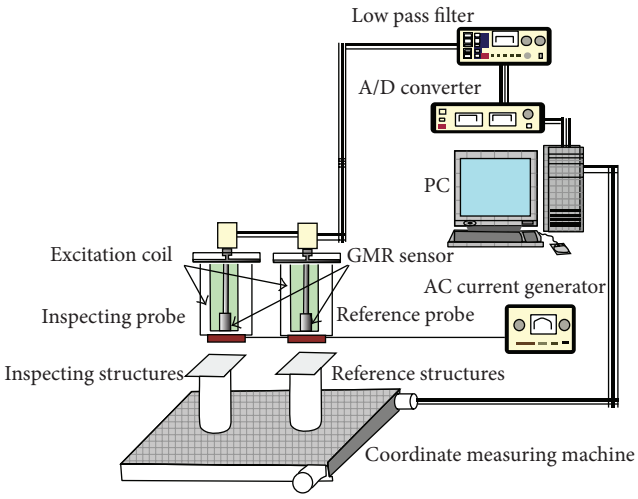

Figure 2: Schematic view of an automatic ECNDE system.

structures, the system can easily make a decision on structure conditions and usage states.

5.2. Experimental Results. To verify the feasibility of the proposed EC inversion models for estimating dimensions of defects in multilayered structures, comparative experiments are carried out. Detection of deeply buried defects in multilayered airframe joints is widely recognized as an urgent and difficult NDE problem [34]. Multilayered samples resembling a part of the projected wing splice of the aircraft are analyzed. We assume that the shape and position of defects are known in advance. Therefore, this paper mainly discusses the inversion problem of estimating dimensions of defects in multilayered structures to simulate the quantification of internal cracks, corrosions, and local interlayer air gaps in real structures.

The experimental specimen is shown schematically in Figure 3. The specimen consists of three layers of aluminum with a total thickness of 10 mm (2.5, 5, 2.5 mm), electrical conductivity $\sigma = 18.5 \times 10^6$ S/m, magnetic permeability $\mu = \mu_0 = 4\pi \times 10^{-7}$ H/m, length $l = 200$ mm, and width $w = 120$ mm. The layers are bolted together with 5 mm diameter Titanium bolts, whose upper part is conically shaped having a diameter of 8 mm at the surface of the specimen. The second layer contains an exchangeable sheet, in which calibrated rectangular defects with different dimensions have been introduced in the center of the plate. The set of defects are of height 1 mm, five depth values varying from 2.5 mm to 6.5 mm, four length values varying from 1 mm to 4 mm, and four width values varying from 1 mm to 4 mm with step 1 mm. A dataset with 80 records is acquired during the scanning. Of the overall 80 samples, we randomly extract 50 samples and use them as the training (calibration) set. The remaining 30 samples are used as the validation set for testing the model. To ensure a fair comparison, the same calibration and validation sets are used for each model. The skin depth $\delta = (\sqrt{\pi f \mu \sigma})^{-1}$ is equal to about 8.28 mm and indicates promising robustness of inspection of all inner defects in the multilayered structures.

The data set is denoised by the WPA method. After the signals are denoised, all the data are mean-centered and scaled to unit variance before modeling. Then, the presented approaches are implemented to construct the inversion models for estimating dimensions of defects, respectively.

Firstly, the PLS regression method is used to construct the calibration model of defect dimension estimation. The PLS components are computed as certain linear combinations of the measured GMR sensor's output signals. The optimal number of PLS components is determined by implementing leave-one-out cross-validation. In cross-validation, the $Q_h{}^2$ of each component of the PLS regression calibration model is illustrated in Figure 4. It shows that the model has seven significant components. This gives a strong indication that seven PLS components are appropriate for modeling. Then, the corresponding defect dimensions are predicted linearly based on these extracted components. Thus, the final predictive function is also a linear combination of the measured GMR sensor's output signals. Figure 5 shows the model overview plot of the cumulative R^2, the fraction of the variation of $\mathbf{Y}$ (all

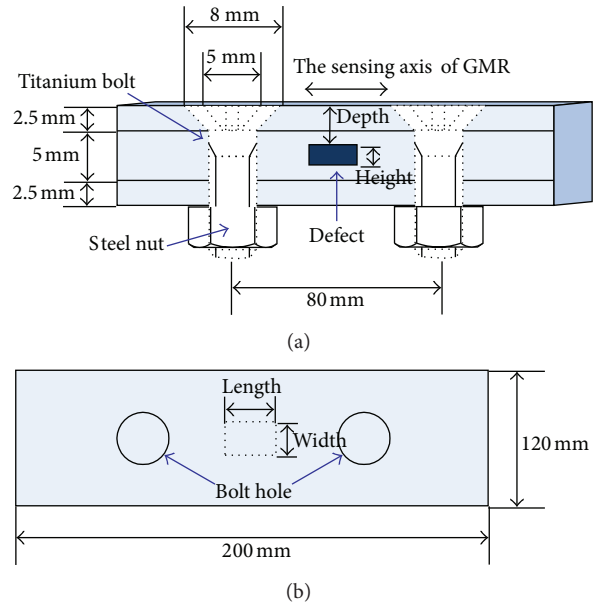

Figure 3: The sketch of an experimental aircraft multilayered structure: (a) cutaway view of the whole structure; (b) vertical view of the second layer.

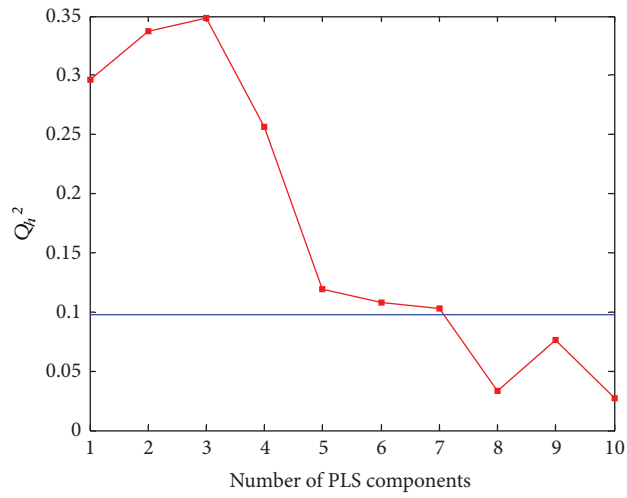

Figure 4: The $Q_h{}^2$ of each component of the PLS regression model.

the responses) explained by the model after each component from the training set, and the cumulative Q^2, the fraction of the variation of $\mathbf{Y}$ (all the responses) explained by the model after each component from the testing set. Values of the cumulative R^2 and Q^2 are higher than 0.8, which indicates the model is appropriate.

Secondly, the KPLS regression method is used to construct the calibration model of defect dimension estimation. In KPLS regression, a radial basis kernel is employed as the kernel function. The same leave-one-out cross-validation procedure is implemented to choose the optimal number of KPLS components. Figure 6 shows the $Q_h{}^2$ of each component of the KPLS regression calibration model. From

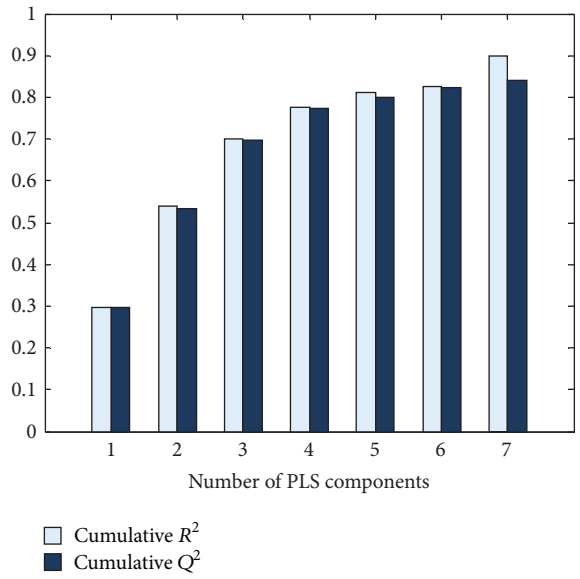

Figure 5: The cumulative R^2 and Q^2 of the PLS regression model.

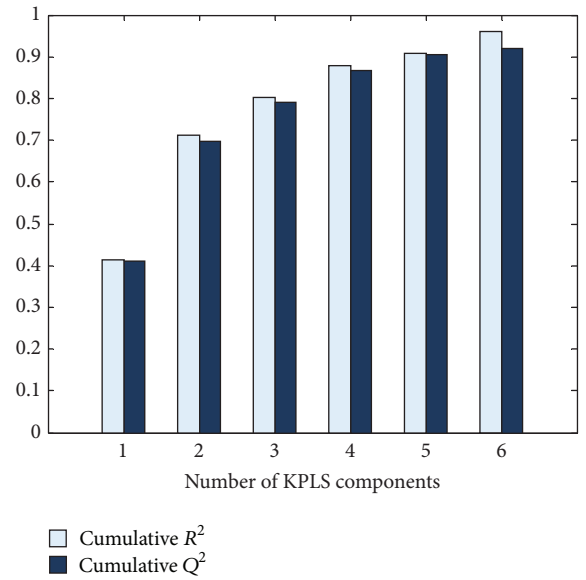

Figure 7: The cumulative R^2 and Q^2 of the KPLS regression model.

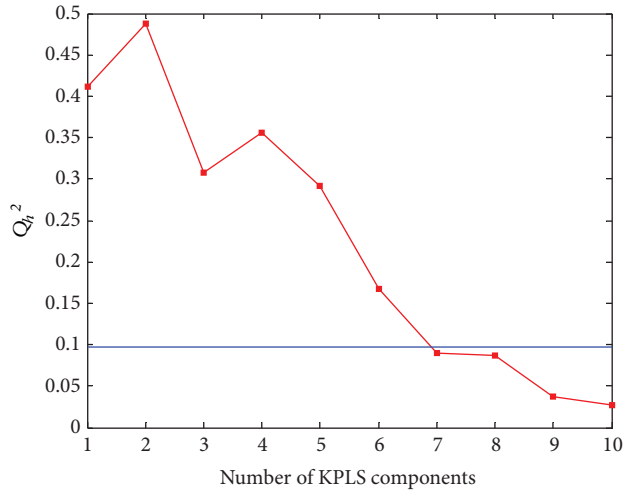

Figure 6: The Q_h^2 of each component of the KPLS regression model.

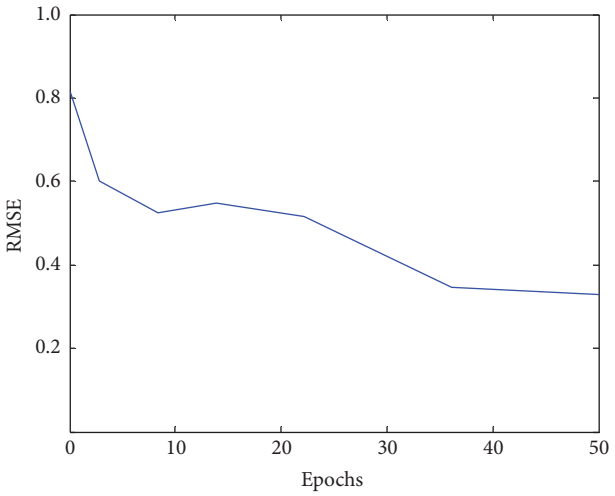

Figure 8: The training curve of ANN.

Figure 6, we can see that the model only has six significant components. Figure 7 shows the model overview plot of the cumulative R^2 and Q^2. Values of the cumulative R^2 and Q^2 are close to 1.0, which indicates that the model is an excellent model.

In addition, in the experiments' tests, a performance comparison between the proposed two methods and the ANN method is carried out. We use a feed-forward neural network with one hidden layer containing 12 neurons. The number of neurons of input layer and output layer is dependent upon the dimensions of X (GMR sensor's output voltage) and Y (defect dimensions), respectively. Then, the training data subset is used for updating the network weight and bias. During training, the error is evaluated in terms of RMSE. The training curve of ANN is shown in Figure 8. Error with respect to the testing data subset is not monitored during training but is quantified to assess the final performance of the trained ANN model.

Finally, to compare the prediction qualities of the three approaches, Figure 9 plots the estimated values obtained from the three approaches against the actual values of defect dimensions of the testing set. The main results obtained from the three inversion models for the training set and the testing set are summarized in Table 2.

From Figure 9 and Table 2, it can be seen that the proposed two methods can gain a better prediction performance than the ANN method. The defect dimension estimation from the proposed two inversion models is more accurate and robust. Among three inversion models, the ANN model gives better prediction results for the training set than those for the testing set, indicating that the ANN model can easily lead to overfitting of the training data and will give

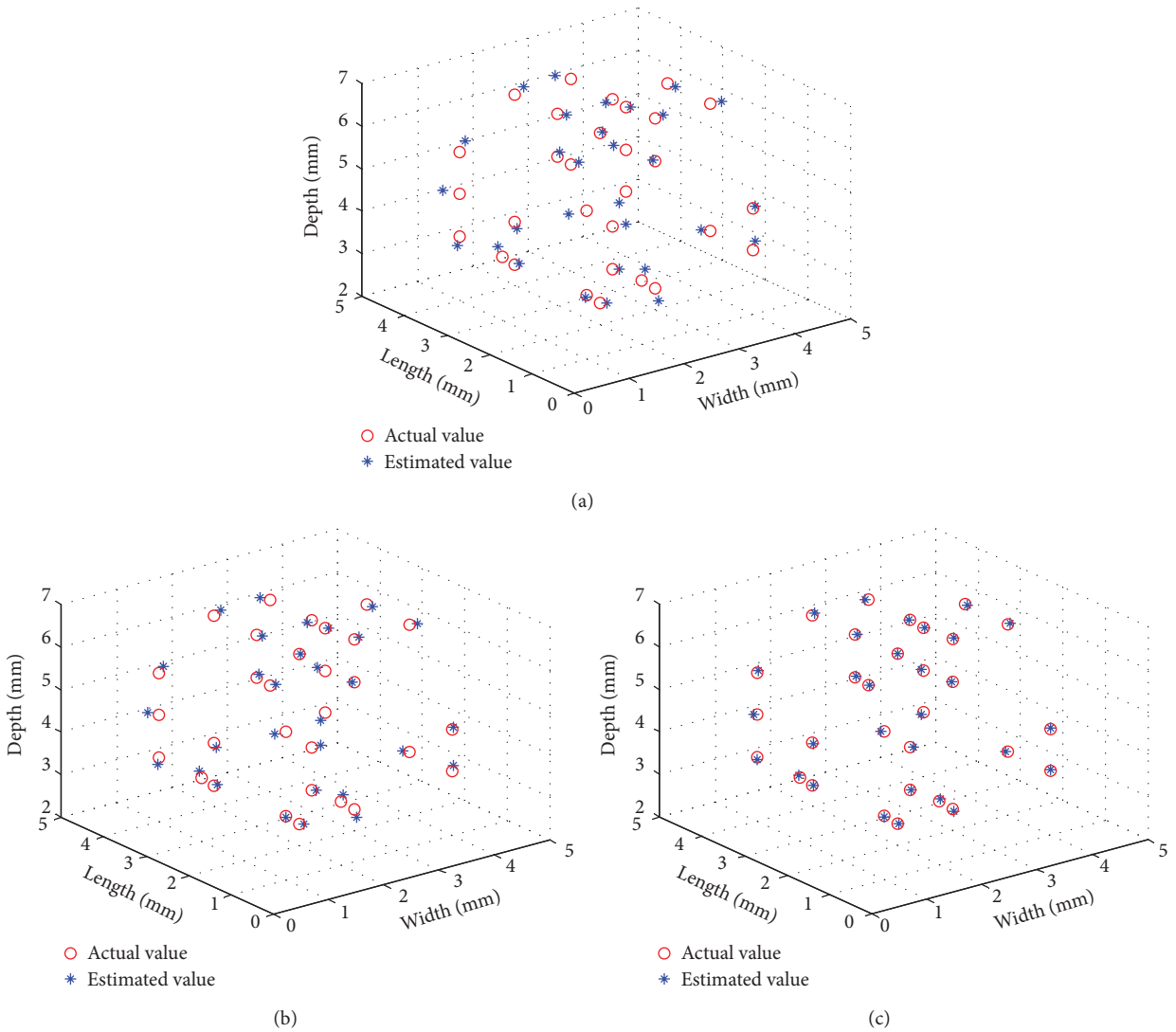

Figure 9: Scatter plots of the actual values versus the estimated values of defect dimensions of the testing set: (a) the ANN method, (b) the PLS regression method, and (c) the KPLS regression method.

obvious errors when the samples have never been contained in the training set. In the PLS regression model, the optimal number of PLS components selected by implementing the cross-validation procedure simplifies the PLS model and enhances the predictive ability of the model. Despite the fact that the PLS model shows a slightly lower fitting of the training data, it has a better prediction ability than the ANN model. Compared to the PLS regression model, the KPLS regression model needs less number of components selected to construct the calibration model, which make the complexity of the model further reduced. When the KPLS regression is used to approximate the model, R^2 and Q^2 are greatly increased, and RMSEC and RMSEP are reduced. The increased prediction performance of the KPLS regression model could be explained by the fact that the ECNDE is an inherently nonlinear process and the KPLS model could capture the nonlinearities in the original data space benefiting from the linear data structure in the feature space. This special property of the KPLS regression may be considered as a more proper way to interpret the nonlinear and nonstationary ECNDE signals.

6. Conclusions

In this study, two EC inversion models for estimating dimensions of defects in multilayered structures are proposed and investigated. The WPA denoising method removes the influence of noise and information not correlated to the target parameter, which effectively improves the performance of the proposed approaches when using time-domain signals. Then, the PLS regression and KPLS regression inversion models are constructed to estimate defect dimensions, respectively. The PLS regression provides an approach to the quantitative modeling for estimating defect dimensions, where the correlation structure of the acquired EC inspection data is considered. The cross-validation is implemented to choose the optimal

Table 2: Main results obtained with the ANN, PLS regression and KPLS regression methods.

Data sets			ANN	PLS	KPLS
Training set	Length	R^2	0.915	0.911	0.986
		RMSEC	0.316	0.323	0.128
	Width	R^2	0.907	0.887	0.931
		RMSEC	0.338	0.372	0.291
	Depth	R^2	0.929	0.902	0.966
		RMSEC	0.381	0.448	0.264
Testing set	Length	Q^2	0.705	0.858	0.953
		RMSEP	0.598	0.412	0.235
	Width	Q^2	0.691	0.821	0.894
		RMSEP	0.611	0.471	0.358
	Depth	Q^2	0.712	0.841	0.916
		RMSEP	0.618	0.573	0.415

number of PLS components to obtain a model with the appropriate complexity and good predictive ability. The KPLS regression is one type of nonlinear PLS regression. Compared with other nonlinear methods, the KPLS regression has the advantage that it does not require a nonlinear optimization procedure. It involves calculations as simple as those used for the PLS regression. At the same time, in comparison to the PLS regression, the KPLS regression uses a smaller number of components.

To test the proposed two inversion models, a strict experiment has been carried out. Two approaches are compared with the ANN method in terms of model's ability to fit data, predictive accuracy, and robustness. Experimental results show that the proposed two approaches can provide better estimation performance than the conventional approaches (the ANN method) in aspects of estimation accuracy, generalization capability, robustness, and computational burden. The results demonstrate the feasibility and effectivity of the proposed two inversion models. They all give the accurate estimation of dimensions of defects in multilayered structures. Between them, the KPLS gives a better prediction performance. The algorithms' capability of quantitative evaluation of defects in multilayered structures is fairly general and fruitful, as this encourages the attempts to tackle the problem of other evaluation problems. In fact, it is necessary to note that, in this paper, we assume that the shape and position of defects are known in advance. However, in most real industrial environments, this hypothesis is not always met. We usually do not know the shape and position of defects in advance. Moreover, in the real ECNDE problems, defects to be detected are usually smaller than the ones considered in the experiments and the shape of defects is very abnormal. Future work, hopefully, will be done to extend the proposed methods to the more complex ECNDE problems where the kind of defect is more general and the smaller abnormal defects are considered.

Conflict of Interests

The authors declare that there is no conflict of interests regarding the publication of this paper.

Acknowledgments

This work is supported by the National Natural Science Foundation of China Grant nos. 51105183 and 51307172, the Research Fund for the Doctoral Program of Higher Education of China Grant no. 20115314120003, the Applied Basic Research Programs of Science and Technology Commission Foundation of Yunnan Province of China Grant no. 2010ZC050, the Foundation of Yunnan Educational Committee Grant no. 2013Z121, the National College Student Innovation Training Program Funded Projects Grant no. 201210674014, and the Science and Technology Project of Yunnan Power Grid Corporation Grant no. K-YN2013-110.

References

[1] A. L. Jones and K. F. Pezdirtz, "Nondestructive eddy current testing," *IEEE Transactions on Instrumentation and Measurement*, vol. 21, no. 1, pp. 11–15, 1972.

[2] H. Zhang, H. C. Yan, F. W. Yang, and Q. J. Chen, "Quantized control design for impulsive fuzzy networked systems," *IEEE Transactions on Fuzzy Systems*, vol. 19, no. 6, pp. 1153–1162, 2011.

[3] H. Zhang, H. C. Yan, F. W. Yang, and Q. J. Chen, "Distributed average filtering for sensor networks with sensor saturation," *IET Control Theory & Applications*, vol. 7, no. 6, pp. 887–893, 2013.

[4] B. A. Auld and J. C. Moulder, "Review of advances in quantitative eddy current nondestructive evaluation," *Journal of Nondestructive Evaluation*, vol. 18, no. 1, pp. 3–36, 1999.

[5] H. C. Yan, Z. Z. Su, H. Zhang, and F. W. Yang, "Observer-based H-infinity control for discrete-time stochastic systems with quantization and random communication delays," *IET Control Theory & Applications*, vol. 7, no. 3, pp. 372–379, 2013.

[6] H. L. Libby, *Introduction To Electromagnetic Nondestructive Test Methods*, John Wiley & Sons, New York, NY, USA, 1971.

[7] A. M. Armour, "Eddy current and electrical methods of crack detection," *Journal of Scientific Instruments*, vol. 25, no. 6, pp. 209–210, 1948.

[8] W. Cheng, S. Kanemoto, I. Komura, and M. Shiwa, "Depth sizing of partial-contact stress corrosion cracks from ECT signals," *NDT & E International*, vol. 39, no. 5, pp. 374–383, 2006.

[9] J. R. Bowler, "Review of eddy current inversion with application to nondestructive evaluation," *International Journal of Applied Electromagnetics and Mechanics*, vol. 8, no. 1, pp. 3–16, 1997.

[10] H. C. Yan, H. B. Shi, H. Zhang, and F. W. Yang, "Quantized H-infinity control for networked delayed systems with communication constraints," *Asian Journal of Control*, vol. 5, no. 5, pp. 1468–1476, 2013.

[11] H. J. Gao, T. W. Chen, and J. Lam, "A new delay system approach to network-based control," *Automatica*, vol. 44, no. 1, pp. 39–52, 2008.

[12] L. X. Zhang, H. J. Gao, and O. Kaynak, "Network-induced constraints in networked control systems-a survey," *IEEE Transactions on Industrial Informatics*, vol. 9, no. 1, pp. 403–416, 2013.

[13] R. C. Popa and K. Miya, "Approximate inverse mapping in ECT, based on aperture shifting and neural network regression," *Journal of Nondestructive Evaluation*, vol. 17, no. 4, pp. 209–221, 1998.

[14] N. Yusa, W. Cheng, Z. Chen, and K. Miya, "Generalized neural network approach to eddy current inversion for real cracks," *NDT & E International*, vol. 35, no. 8, pp. 609–614, 2002.

[15] M. Davoust, L. L. Brusquet, and G. Fleury, "Robust estimation of flaw dimensions using remote field eddy current inspection," *Measurement Science and Technology*, vol. 17, no. 11, pp. 3006–3014, 2006.

[16] J. Rosa, G. Fleury, E. O. Sonia, and M. Davoust, "Markov chain Monte Carlo posterior density approximation for a groove-dimensioning purpose," *IEEE Transactions on Instrumentation and Measurement*, vol. 55, no. 1, pp. 112–122, 2006.

[17] J. Rosa and G. Fleury, "Bootstrap methods for a measurement estimation problem," *IEEE Transactions on Instrumentation and Measurement*, vol. 55, no. 3, pp. 820–827, 2006.

[18] K. Krzywosz, "Enhanced Id pit sizing using multivariate regression algorithm," *Review of Progress in Quantitative Nondestructive Evaluation*, vol. 26, pp. 741–748, 2007.

[19] A. Bernieri, L. Ferrigno, M. Laracca, and M. Molinara, "Crack shape reconstruction in eddy current testing using machine learning systems for regression," *IEEE Transactions on Instrumentation and Measurement*, vol. 57, no. 9, pp. 1958–1968, 2008.

[20] T. Dogaru and S. T. Smith, "Giant magnetoresistance-based eddy-current sensor," *IEEE Transactions on Magnetics*, vol. 37, no. 5, pp. 3831–3838, 2001.

[21] F. C. Morabito, "Wavelet tools for improving the accuracy of neural network solution of electromagnetic inverse problems," *IEEE Transactions on Magnetics*, vol. 34, no. 5, pp. 2964–2967, 1998.

[22] H. Wold, "Path models with latent variables: the NIPALS approach," in *Quantitative Sociology: International Perspectives on Mathematical and Statistical Modeling*, pp. 307–357, Academic, New York, NY, USA, 1975.

[23] S. Wold, M. Sjöström, and L. Eriksson, "PLS-regression: a basic tool of chemometrics," in *Chemometrics and Intelligent Laboratory Systems*, vol. 58, pp. 109–130, 2001.

[24] R. J. Rosipal and L. Trejo, "Kernel partial least squares regression in reproducing kernel Hilbert space," *Journal of Machine Learning Research*, vol. 2, no. 6, pp. 97–123, 2001.

[25] K. Kim, J. M. Lee, and I.-B. Lee, "A novel multivariate regression approach based on kernel partial least squares with orthogonal signal correction," *Chemometrics and Intelligent Laboratory Systems*, vol. 79, no. 1-2, pp. 22–30, 2005.

[26] S. Norton and J. R. Bowler, "Theory of eddy current inversion," *Journal of Applied Physics*, vol. 73, no. 2, pp. 501–512, 1993.

[27] M. H. Kutner, C. J. Nachtsheim, and J. Neter, *Application Linear Regression Models*, McGrew-Hill, 4th edition, 2004.

[28] Y. J. Chen, Y. W. Shi, and Y. P. Lei, "Use of a wavelet analysis technique for the enhancement of signal-to-noise ratio in ultrasonic NDE," *Insight: Non-Destructive Testing and Condition Monitoring*, vol. 38, no. 11, pp. 800–803, 1996.

[29] I. Daubechies, S. Mallat, and A. S. Willsky, "Introduction to the special issue on wavelet transforms and multiresolution signal analysis," *IEEE Transactions on Information Theory*, vol. 38, pp. 529–532, 1992.

[30] S. Wold, "Discussion: PLS in chemical practice," *Technometrics*, vol. 35, pp. 136–139, 1993.

[31] S. Rännar, F. Lindgren, P. Geladi, and S. Wold, "A PLS kernel algorithm for data sets with many variables and fewer objects—part 1: theory and algorithm," *Journal of Chemometrics*, vol. 8, pp. 111–125, 1994.

[32] I. N. Wakeling and J. J. Morris, "A test of significance for partial least squares regression," *Journal of Chemometrics*, vol. 7, no. 4, pp. 291–304, 1993.

[33] F. Pérez-Cruz and O. Bousquet, "Kernel methods and their potential use in signal processing," *IEEE Signal Processing Magazine*, vol. 21, no. 3, pp. 57–65, 2004.

[34] T. Dogaru, C. H. Smith, R. W. Schneider, and S. T. Smith, "Deep crack detection around fastener holes in airplane multi-layered structures using GMR-based eddy current probes," *Review of Progress in Quantitative Nondestructive Evaluation*, vol. 23, pp. 398–405, 2004.